A&A 446, 603–609 (2006)
DOI: 10.1051/0004-6361:20053219

Astronomy & Astrophysics

An abundance analysis of the symbiotic star CH Cygni⋆

M. R. Schmidt[1], L. Začs[2], J. Mikołajewska[3], and K. H. Hinkle[4]

[1] N. Copernicus Astronomical Center, ul. Rabiańska 8, 87-100 Toruń, Poland
e-mail: schmidt@ncac.torun.pl
[2] Institute of Atomic Physics and Spectroscopy, University of Latvia, Raiņa bulvāris 19, 1586 Rīga, Latvia
e-mail: zacs@latnet.lv
[3] N. Copernicus Astronomical Center, ul. Bartycka 18, 00716 Warsaw, Poland
e-mail: mikolaj@camk.edu.pl
[4] National Optical Astronomy Observatory, PO Box 26732, Tucson, AZ 85726, USA
e-mail: hinkle@noao.edu

Received 9 April 2005 / Accepted 12 September 2005

ABSTRACT

The photospheric abundances for the cool component of the symbiotic star were calculated for the first time using high-resolution near-infrared spectra and the method of of standard LTE analysis and atmospheric models. The iron abundance for CH Cyg was found to be solar, [Fe/H] = 0.0 ± 0.19. The atmospheric parameters ($T_{\rm eff}$ = 3100 K, $\log g$ = 0.0 (cgs), $\xi_{\rm t}$ = 2.2 km s^{-1}) and metallicity for CH Cyg are found to be approximately equal to those for nearby field M7 giants. The calculated [C/H] = −0.15, [N/H] = +0.16, [O/H] = −0.07, and the isotopic ratios of ^{12}C/^{13}C and ^{16}O/^{17}O are close to the mean values for single M giants that have experienced the first dredge-up. A reasonable explanation for the absence of barium star-like chemical peculiarities seems to be the high metallicity of CH Cyg. The emission line technique was explored for estimating CNO ratios in the wind of the giant.

Key words. binaries: symbiotic – stars: abundances – stars: late-type – stars: individual: CH Cyg

1. Introduction

Both symbiotic and peculiar red giants (barium, CH-stars, extrinsic S stars, etc.) are binaries with a cool giant primary and a hot (WD) secondary. Interaction between the binary components results in peculiar chemical composition in the atmospheres of barium and related giants. This is believed to result from the previous transfer of *s*-process rich mass from the AGB star, which is now a WD, to the star that now appears as the red giant (Han et al. 1995; Začs 2000). Symbiotic activity indicates that these binaries are currently interacting. Symbiotic systems also have a white dwarf that was previously an AGB star and a red giant that was a main sequence star during the AGB phase of the now white dwarf. An obvious expectation is that there are red giants with WD companions that are both chemically peculiar and symbiotic (see, for review, Jorissen 2003). Although a number of symbiotic stars are well studied there is a lack of detailed abundance analysis based on high-resolution spectra.

The link between the *yellow* symbiotics and peculiar giants has been established using the abundance patterns (Smith et al. 1996, 1997; Pereira et al. 1998; Smith et al. 2001). All known yellow symbiotic stars studied so far using atmospheric models display significant enhancement of s-process elements, similar to peculiar giants (see, Jorissen 2003). They are clearly halo objects, as revealed by their low metallicities and high space velocities. The s-process Ba and Sr enhancements have been also found in the two symbiotic stars containing a CH-type giant with a very high C overabundance (Schmid 1994). CH stars are also metal poor halo objects.

For the *red* symbiotics a link to the chemically peculiar giants is much more tenuous. Only a small number of galactic red symbiotic stars have a cool carbon-rich star as a cool component. Recently, peculiar chemical composition was confirmed for the red symbiotic HD 35155; the star was found to be metal deficient, [Fe/H] = −0.8, and rich in neutron-capture elements, [n/Fe] = + 2 dex on average (Vanture et al. 2003). It is not clear why among red symbiotic stars the percent of carbon and s-process rich stars is so low.

CH Cyg (=HD 182917 = HIP 95413) is the brightest symbiotic binary at visual wavelengths and the second brightest symbiotic in the 2 μm infrared. The CH Cyg system has been observed both photometrically and spectroscopically from radio through *X*-ray wavelengths. Both the light curves and the radial velocity curves show multiple periodicites (e.g. a ∼100$^{\rm d}$ photometric period best visible in the *VRI* light curves,

⋆ Tables 1 and 2 are only available in electronic form at http://www.edpsciences.org

attributed to radial pulsations of the giant (Mikołajewski et al. 1992), and a secondary period of ~756^{d} also present in the radial velocity curve (Hinkle et al. 1993).

There is a controversy about whether the CH Cyg system is triple or binary system and if triple whether the symbiotic pair is the inner binary or the white dwarf is on the longer orbit (Hinkle et al. 1993; Munari et al. 1996). Although the triple-star model is very appealing, this model does not easily explain the observed photometric behaviour (Munari et al. 1996, and references therein). Recent study of radial velocity variations of nine multiple-mode semiregular M-giants (SRVs) revealed radial-velocity periods longer than the fundamental radial mode in six of the nine giants (Hinkle et al. 2002). Although the authors considered a possibility that the velocity variations are due to orbital motion, the nearly identical orbital parameters (K, e, and to a lesser extent also ω) for five of the six SRVs make a binary model very unlikely. As discussed by Wood et al. (2004) and Hinkle et al. (2002) evidence points to a stable non-radial pulsation of very long period rather than duplicity. The orbital parameters, K, e, ω, for the ~756^{d} pair of CH Cyg (Hinkle et al. 1993) are practically the same as those for these five multiple-period SRVs studied by Hinkle et al. (2002). This strongly suggests that the ~756^{d} period in CH Cyg is a non-radial pulsation mode. If so, the ~5300^{d} velocity variation discussed by Hinkle et al. (1993) must then be the symbiotic orbit.

The cool giant has been classified as M7 (M6.5–M7.5) by Mürset & Schmid (1999). In a quiet phase the cool component is a typical oxygen-rich star with TiO bands dominating the red region of the optical spectrum. In the past CH Cyg was used as a M6 spectral standard (Keenan 1963). Chemical peculiarities are not obvious in the optical spectrum of CH Cyg. However, due to the crowded spectrum in the optical spectral region an analysis of chemical composition is very difficult. Here for the first time we present a detailed abundance analysis of CH Cyg based on high-resolution, near-infrared spectra, the method of standard LTE analysis and atmospheric models, and spectrum synthesis. We have also looked for variations of selected absorption lines.

2. Observations and data reduction

The high-resolution 2 μm region spectra of CH Cyg were obtained with the Fourier transform spectrometer (FTS) at the coudé focus of the KPNO Mayall 4 m telescope (Hall et al. 1978) between 1979 and 1992. The majority of the observations were taken with either a K filter (2.0–2.5 μm) or a broad-band 1.5–2.5 μm filter covering both the K and H bands. The resolution of the spectra is 0.07 cm^{-1} (~4 km s^{-1}). The typical signal-to-noise (S/N) ratio of the spectra selected for abundance analysis range from 80 to 180 around 4600 cm^{-1} and twice less in the H-band. For more details about observations and reduction of the data see Hinkle et al. (1993).

The six spectra of CH Cyg were selected for further analysis in this paper. Five of them are in the K band where the spectrum is less crowded and the continuum seems to be clearly defined. To cover different phases of symbiotic activity the spectra observed on 11 June 1982, 30 December 1984, 14 March 1987, 15 May 1987, and 6 April 1991 were chosen. In addition one spectrum observed on 13 January 1989 in H band was selected for abundance analysis. All the selected spectra have high S/N ratio and low level of fringing visible in some of the 46 spectra available.

2.1. Identification and measurements of absorption lines

An inspection of the selected spectra of CH Cyg shows that a large number of lines for neutral atoms (Na, Mg, Al, Si, S, Ca, Sc, Ti, V, Cr, Fe, Ni) and molecules (CO, CN, OH, HF) are evident. Also some lines of H_2O were found near 4700 cm^{-1} using the list of sunspot water lines identified by Wallace et al. (1996). To our knowledge no s-process element abundances have been studied in H and K bands. The line databases used in the paper contain few lines of Ba I and Y I in the spectral regions of interest with these lines too weak to be identified. Strong enhancements, >1 dex, would be necessary to enable clear identification of these lines in the spectrum.

Absorption line identifications were made using the list of atomic lines given by Mélendez & Barbuy (1999) in the H band, the VALD database in the K band (Kupka et al. 1999) and the atlas of cool stars spectra prepared by Wallace & Hinkle (1996). The molecular lines were identified using the line list of CO and isotopic vibration-rotation transitions given by Goorvitch & Chackerian (1994), HF transitions prepared by Jorissen et al. (1992), molecular data from Kurucz (1995) and the list of red system CN lines published by Davis & Phillips (1963).

No telluric reference spectra were taken for these CH Cyg observations and hence it was not possible to remove telluric lines from the spectra. However, this prove not to be a serious limitation because many stellar lines are uncontaminated by telluric features. Therefore the first task was to identified stellar and telluric lines in the observed spectra of CH Cyg. An atmospheric transmission function adopted from the Arcturus Atlas (Hinkle et al. 1995) was used to select stellar lines whose positions differ significantly from telluric features. In total more than 300 clean atomic and molecular lines for abundance analysis were selected, however, only a part of them have acceptable spectral line data. Equivalent widths (EW) of selected lines were measured by fitting with the Gaussian using the standard DECH20T routine (Galazutdinov 1992) both in the spectra of CH Cyg and the Sun. Equivalent widths measured at different phases of stellar activity were compared. Only a small fraction of the equivalent widths displayed significant changes, i.e. more than 10%. We are not sure that these changes are due to physical effects. The variations in EW could be because of uncertainties in the continuum definition and contamination by neglected telluric components. Notice that the locations of telluric lines change in the spectra with both heliocentric velocity and orbital phase. Additional analysis is needed to understand nature of changes in some EW. In this paper only constant stellar lines are exploited. In the final list of lines for abundance analysis (see Tables 1 and 2) clean absorption lines with acceptable atomic (molecular) data were included and averaged equivalent widths are given.

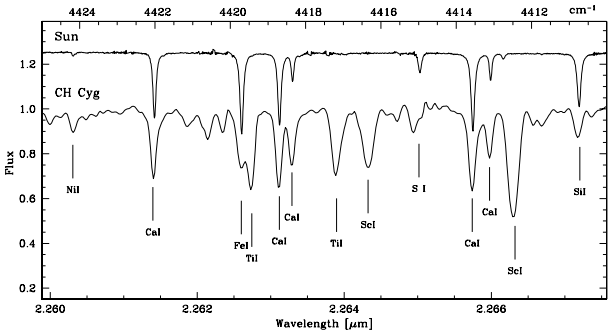

Fig. 1. The observed spectrum of CH Cyg in the region of well-known Ca index. Also shown is the spectrum of the Sun (Wallace et al. 1996).

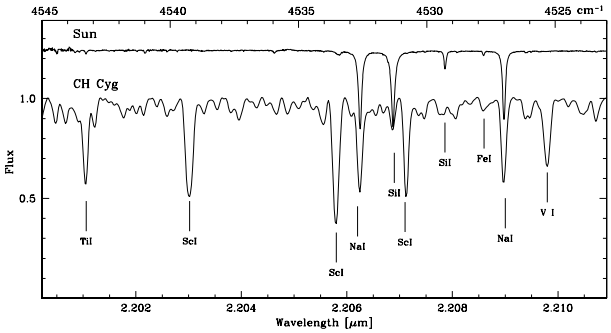

Fig. 2. Same as Fig. 1, but around the Na index.

Although normalization of spectra sometimes is difficult the abundance calculations for iron over the observed spectral region gives evidence that in general the continuum is clearly defined. Notice that the spectrum of CH Cyg in the *H* band is much more crowded than in the *K* band. Therefore for abundance calculations we prefer the *K* band. In the *K* band it is also easier to detect fringing as a modulation of the continuum. The resulting rectified spectra for two typical wavelengths regions are presented in Figs. 1 and 2. Also shown is the spectrum of the Sun (Wallace et al. 1996) which we used to check the methodology of abundance calculations.

3. Analysis and results

The standard LTE line analysis program WIDTH9 developed by R. L. Kurucz has been employed for abundance calculations of atomic lines. Model atmospheres were extracted from Hauschildt et al. (1999). The most recent version of the spectrum synthesis code MOOG (Sneden 1973) was used for analysis of selected molecular lines. Spectral lines stronger than 300 mÅ were not used in general for abundance calculations. The abundances using the same sample of lines were calculated for CH Cyg and the Sun to detect possible systematic effects. For solar atmosphere the Kurucz's model (Kurucz 1993) of the Sun was adopted. The calculations of synthetic spectra over the entire observed spectral region were done using the code WIDMO developed by one of us (M.S.).

3.1. Atmospheric parameters

The effective temperature of CH Cyg was estimated by Dyck et al. (1999) using interferometric measurements of the angular diameter, $T_{\rm eff} = 3084 \pm 130$ K. Effective temperature as a function of spectral type for M giants was calibrated by Richichi et al. (1999) using lunar occultation measurements corrected by inclusion limb darkening effects. According to this calibration spectral type M7 corresponds to an effective temperature of 3150 ± 95 K. Photometric estimation of temperature is rather difficult for CH Cyg because of the variability of colour indexes. The temperature $T_{\rm eff} = 3100$ K seems to be good approximation for this cool giant.

The surface gravity ($\log g$) for CH Cyg is not possible to determine in the standard way from the Fe I/Fe II ionization balance due to absence of detectable lines of ions in the cool atmosphere of giant. Molecular lines are not useful for this task because partial pressures are not sensitive to the total pressure. Surface gravity may be found from the trigonometric parallax, $\pi = 3.73 \pm 0.85$ mas (ESA 1997). Using this value, $m_{\rm V}$ from 7.40 to 9.10 mag (SIMBAD), $BC = -4.42$, $T_{\rm eff} = 3100$ K and adopting a mass of $M = 2\ M_{\odot}$ the standard relation

$$\log g = 4 \log T_{\rm eff}/T_{\odot} + \log M/M_{\odot} + 2 \log \pi + 0.4(V + BC - 0.26) + 4.44$$

leads to $\log g$ from -0.1 to $+0.6$ (cgs). This estimation is close to the standard value of 0.0 for M7 giants (Houdashelt et al. 2000).

The microturbulent velocity for CH Cyg was estimated by forcing the abundances of the individual Fe I lines to be independent of the equivalent widths, $\xi_t = 2.2$ km s^{-1}. The macroturbulent velocity was introduced in order to fit the profiles of synthesized and observed lines. The *FWHM* value of 5.9 km s^{-1} was measured using a number of weak symmetric lines. Notice that Hinkle et al. (1993) found a variability of *FWHM* during the short-period orbital motion.

The atmospheric parameters adopted for abundance calculations of CH Cyg are as follows: $T_{\rm eff} = 3200$ K, $\log g = 0.0$ (cgs), and $\xi_t = 2.2$ km s^{-1}, nearest in the grid of model atmospheres (Hauschildt et al. 1999) and close to the mean values for single M giants (Houdashelt et al. 2000). Uncertainties in the adopted atmospheric parameters were estimated to be ± 200 K in temperature, ± 0.5 dex in gravity and ± 0.5 km s^{-1} in microturbulent velocity. For the Sun standard atmospheric parameters (5777 K, 4.44 (cgs), 1.0 km s^{-1}) were accepted.

3.2. Atomic and molecular data

The insufficient quality of available atomic and molecular data is a serious limitation for abundance analysis using lines in the infrared spectral region. The abundances of Mg, Si, Ti, Fe, and Ni in this paper were calculated using atomic lines. The atomic data for measured lines were collected using the VALD database (Kupka et al. 1999) and the list prepared by Mélendez & Barbuy (1999). The quality of the collected oscillator strengths was inspected via abundance calculations of the Sun. Unfortunately, not all lines selected and measured in the spectrum of CH Cyg are detectable in the spectrum of Sun.

The solar abundance of Fe I was calculated using lines in the CH Cyg line list. Abundances from individual lines were compared to the mean and lines giving incorrect values were omitted. An average metallicity of the Sun was found to be 7.54 ± 0.12 (see Table 3) from the best lines, close to that obtained in the optical region, 7.50 ± 0.12 (Grevesse & Sauval 1998). Then the same sample of lines with the same ($\log gf$) was used to calculate the iron abundance of CH Cyg. This minimized the role of systematic effects (see the last column in Table 3).

The same methodology was used to select lines of Mg I, Si I, Ti I, and Ni I with best available oscillator strengths. The solar abundances of these elements, calculated using these lines, are presented in Table 3. The systematic effects and standard deviations in abundances mainly due to errors in $\log gf$ are in general lower than those due to uncertainties in the atmospheric parameters for CH Cyg (see Table 4). Unfortunately, our efforts to create a sample of lines with acceptable oscillator strengths for Na I, Al I, S I, Ca I, Sc I, V I, Cr I was unsuccessful mostly due to serious problems with quality of oscillator strengths for these elements in the infrared.

The abundances of CNO elements and fluorine were calculated using the molecular lines. The vacuum wavelengths, excitation potentials, and gf-values for the vibration-rotation lines of CO isotopes are adopted from Goorvitch (1994). Both $\Delta v = 2$ second overtone lines in K-band and $\Delta v = 3$ third overtone lines in H-band were involved in the analysis. The accepted dissociation energy of CO was $D_0 = 11.091$ eV. In the case of ^{12}CO, ^{13}CO, ^{12}CN, and OH lines the list of lines used by Smith & Lambert (1990) was adopted. The abundance of fluorine was calculated using rotation-vibration lines of HF molecule. HF data given by Jorissen et al. (1992) were used.

3.3. Abundances

The mean absolute and relative abundances in the scale of $\log \varepsilon(\mathrm{H}) = 12.0$ derived with $T_{\rm eff} = 3200$ K, $\log g = 0.0$, $\xi_{\rm t} = 2.2$ km s^{-1} and [M/H] = 0.0 for CH Cyg are given in Table 3, together with the standard deviations of abundances estimated from individual lines, and the number (n) of lines used in the analysis. The abundances relative to the Sun ([X]) were calculated using solar photospheric data provided by Grevesse & Sauval (1998), except in the case of fluorine, for which we used the meteoritic solar abundance of 4.48. The systematic errors in abundances produced by uncertainties in $T_{\rm eff}$ (±200 K), $\log g$ (±0.5 dex), and ξ_t (±0.5 km s^{-1}) would lead to errors, less than 0.3 dex for all elements (see Table 4).

3.4. Isotopic ratios

The high resolution spectra provide an opportunity to estimate the isotopic ratios of carbon and oxygen using individual lines of ^{13}C^{16}O, ^{12}C^{17}O and ^{12}C^{18}O. The spectral region redward of the ^{13}CO (2–0) band head is significantly contaminated by telluric lines. However, nine clean ^{13}C^{16}O lines (Table 2) were selected between the band heads of the systems (2–0) ^{13}C^{16}O and (4–2) of ^{12}C^{16}O. The ratio ^{12}C/^{13}C was calculated to be 18^{+12}_{-6}.

A relatively uncontaminated sample of ^{12}C^{17}O lines was identified in the spectral range from 4278 to 4294 cm^{-1}. This region also has a number of strong telluric lines. To check clean profiles the spectrum was rationed by the logarithmically corrected telluric spectrum from the Arcturus Atlas. In addition, the synthetic spectrum was calculated over the entire range to see possible contamination by other molecular (^{12}C^{16}O, CN) lines in the stellar spectrum. Eight clean ^{12}C^{17}O lines were selected and measured (see Table 2) and the ^{16}O/^{17}O ratio was estimated to be 830^{+400}_{-270}.

Due to the complex telluric spectrum the selection of clean lines in the region of (2–0) ^{12}C^{18}O band head was problematic. A crude estimate of the ^{16}O/^{18}O isotopic ratio was made using the spectral synthesis method, ^{16}O/^{18}O > 1000.

Table 3. Averaged absolute and relative abundances for CH Cyg and the Sun calculated using the same sample of absorption lines. The standard deviations and the number of lines used in the analysis are also given.

	CH Cyg			Sun		
X	$\log \epsilon(X)$	n	$[X]$	$\log \epsilon(X)$	n	$[X]$
C	8.37 ± 0.22	11	−0.15			
N	8.08 ± 0.13	13	+0.16			
O	8.76 ± 0.24	15	−0.07			
F	4.65 ± 0.15	4	+0.17			
Mg	8.68 ± 0.21	10	+1.10	7.40 ± 0.12	4	−0.18
Si	7.40 ± 0.18	13	−0.15	7.43 ± 0.24	11	−0.12
Ti	5.24 ± 0.09	7	+0.22	5.05 ± 0.19	6	+0.03
Fe	7.50 ± 0.19	51	+0.00	7.54 ± 0.12	51	+0.04
Ni	6.65 ± 0.19	12	+0.40	6.36 ± 0.22	10	+0.11

Table 4. Sensitivity of abundances to uncertainties in stellar parameters.

ΔX	$\Delta T_{\rm eff} = -200$ K	$\Delta \log g = +0.50$	$\Delta \xi_t = +0.5$
C	−0.11	+0.20	−0.11
N	−0.13	−0.25	−0.06
O	−0.26	−0.01	−0.15
F	−0.30	+0.18	−0.13
Ti	−0.20	+0.10	−0.30
Fe	0.07	+0.13	−0.12

4. Discussion

An LTE abundance analysis of the red symbiotic star CH Cyg was made for the first time using high-resolution near-infrared spectra and atmospheric models. Weak and medium strong ($EW < 300$ mÅ) atomic lines formed deeply in the atmosphere of cool giant were used to calculate abundances of iron and α-group elements. The abundance of iron was found to be solar. The mean of three selected iron group elements (Ti, Fe, Ni) displays slight overabundance, [M] = +0.2 dex. Possible uncertainties in atmospheric parameters lead to errors of no more than 0.3 dex for all elements.

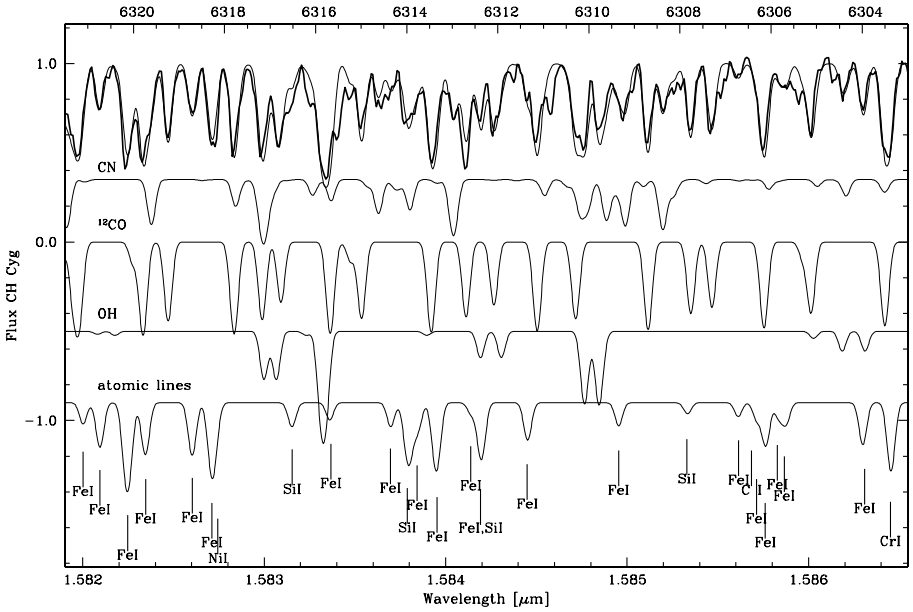

Fig. 3. The observed (thick line) and synthetic spectra calculated using final abundances of the symbiotic star CH Cyg in the spectral region from 1.582 to 1.586 μm are shown on the top. The synthesized CN, OH, ^{12}CO, and atomic components are presented separately. Atomic lines are identified by ticks.

CNO abundances were determined using first and second overtone CO lines, first overtone OH lines, and CN red system lines. [C/H] = −0.15, [N/H] = +0.16 and [O/H] = −0.07, close to the averaged values obtained for single M giants by Smith & Lambert (1990). C/O = 0.40 again in agreement with bright field M giants. The isotopic ratios ^{12}C/^{13}C = 18 and ^{16}O/^{17}O = 830 calculated using isotopic absorption lines also are approximately equal to those for single M giants.

In the standard picture of a symbiotic binary the hot WD component ionizes the cool giant wind giving rise to strong UV emission lines of C III], C IV, N III], N IV] and O III]. Based on emission line fluxes from these ions, Nussbaumer et al. (1988) deduced C/N and O/N abundance ratios for 24 symbiotic systems observed with the *IUE* satellite. They found that the CNO abundance ratios place the symbiotic stars in the transition region from giants to supergiants, almost coinciding with the M-giants. They also noted that their method tends to overestimate nitrogen relative to oxygen and carbon, although the effect is not larger than ∼30%.

Our abundances calculated from the M giant absorption lines can be compared with those derived from the UV emission lines providing an opportunity for a verification of the method used by Nussbaumer et al. (1988), and more generally any method based on emission lines. The fluxes of emission lines for CH Cyg were measured using low resolution *IUE* observations obtained during 1979–1986 by Mikołajewska et al. (1988), to which we added measurements from *IUE* observations through May 1989. The relative abundance of C/N and O/N were determined using 22 observations following the procedure described by Nussbaumer et al. (1988). The average ratios were: C/N = 0.57, O/N = 2.0, and C/O = 0.28. The ratios place CH Cyg among other symbiotic systems in the C/N–O/N plane (cf. Figs. 2–4 of Nussbaumer et al. 1988). However, the standard deviations of the mean values of C/N and O/N are about ∼50%. The standard deviation of the mean C/O ratio is lower, ∼28%. It seems that the fluxes of oxygen and carbon emission lines are changing in phase, while nitrogen emission lines evolved differently.

The mean C/O ratio obtained using emission line techniques is close to that calculated using molecular absorption lines, C/O = 0.4. However, the differences in C/N and O/N ratios between two methods are significant. The molecular absorption lines give higher values, C/N = 1.6 and O/N = 4.0, respectively, and on the C/N–O/N plane place CH Cyg among M giants. An important source of uncertainties in the photospheric abundance analysis is the dissociation energy of CN, D_0^0(CN). For this study, we have adopted D_0^0(CN) = 7.65 eV from Bauschlicher et al. (1988). Adopting a higher value of D_0^0(CN) = 7.77 eV (Costes et al. 1990) would reduce nitrogen abundance by 0.28 dex increasing even more the discrepancy with the emission line results. The N abundance could be increased by adopting a lower value of the surface gravity (see Table 4). However, with the available grid of models, a quantitative analysis of this hypothesis is not yet possible. As long as we assumed correctness of the determination of the nitrogen abudances, this result suggests that at least in case of CH Cyg, the method based on emission lines may overestimate the abundance of nitrogen by a factor of a few. Alternatively, it is possible that in CH Cyg, the emission lines originate in the ejecta/jets from the hot component rather than in the illuminated parts of the M giant wind.

The atlas of spectra of cool stars published by Wallace & Hinkle (1996) provides spectra of two M giants – λ Dra (M0 III) and RX Boo (M8 III) and two M supergiants – α Ori (M2 Ia) and α Her (M5 Ib-II). Qualitative comparison of these spectra shows differences among the spectra of single M (super)giants and the cool giant of CH Cyg. In the spectra of single (super)giants the depth of (2–0) ^{12}C^{16}O band head is about

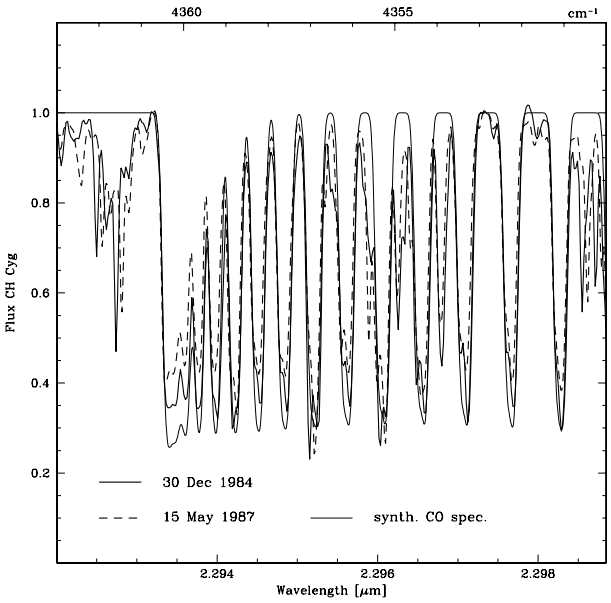

Fig. 4. The observed spectra (thick solid an dashed) of CH Cyg in the region of (2–0) $^{12}C^{16}O$ band head for two different phases of symbiotic activity. Also shown is the calculated spectrum (thin solid) using the final atmospheric parameters and abundances.

65–70%, whereas in CH Cyg the CO band heads are never deeper than 60% (Fig. 4). The same conclusion may be drawn inspecting the strong vibrational-rotational lines of CO bands in the *K* band. A quantitative comparison of the equivalent widths of (2–0) high rotational transitions lines R78–R81 with the data for some M giants (Smith & Lambert 1990) shows that the equivalent widths of these lines measured in CH Cyg (M7) are typical for early M stars. A speculation is that the differences in the CO lines results from the upper atmosphere of CH Cyg cool giant being modified by *X-UV*-radiation of WD companion. However, the spectra chosen for the analysis were taken when the red giant was closer to us than the hot component according to the long period orbit of Hinkle et al. (1993), and the illuminated hemisphere could not be well visible. Moreover, the depth of (2–0) $^{12}C^{16}O$ band head reached the lowest value in 1987–88 when the hot component luminosity reached its minimum value (e.g. Mikołajewska et al. 1993) which could be hardly reconciled with the illumination hypothesis. A caveat is that weakening of the strongest lines has also been seen in spectra of late-type large amplitude variable stars, perhaps as the result of either extended atmospheric layers or mechanical energy transport to the more tenuous regions of the atmosphere, or a combination of these effects (Hinkle et al. 1982).

Another possibility is the presence of the hot dust envelope. In fact, ISO spectra do show the existence of an extended dust envelope around CH Cyg (Schild et al. 1999). Calculations with the DUSTY code (Ivezić & Elitzur 1995, 1997) show that the contribution of the flux from the dust to the total flux at *K* band wavelengths can reach at most a few percent. So this possibility cannot be totally rejected. Perhaps this is supported by the fact that CO bands in *H* band are well reproduced by the synthetic spectrum, and that minimum band depth is coincinding with the maximum of the *M* band light curve of Munari et al. (1996). However, elaboration on this topic is outside the scope of the paper.

To fit the equivalent widths of the lines (2–0) R78–R81 the carbon abundance of CH Cyg would have to be changed by −0.7 dex, in conflict with the carbon abundance calculated from the weak second overtone CO lines. The reason can not to be an error in the effective temperature adopted because we would have to raise the temperature to 3800 K to fit R78–R81 equivalent widths. Such a high effective temperature is inconsistent with the spectroscopic type and colours. Smith & Lambert (1990) discussed in details similar effects for single M giants and concluded that strongest CO lines are not simple monitors of carbon abundance. These lines should be rejected in deriving both the microturbulence and the abundance because the outermost layers where strong lines are formed differ from the model atmosphere. Mechanical heating may lead to higher temperatures and/or microturbulence in the surface layers.

5. Conclusions

1. The photospheric abundances for the cool component of symbiotic star CH Cyg were calculated for the first time using high-resolution, near-infrared spectra and the method of standard LTE analysis and atmospheric models. Iron abundance for CH Cyg was found to be solar, [Fe/H] = +0.0 ± 0.19. The atmospheric parameters, ($T_{\rm eff}$ = 3200 K, $\log g$ = 0.0 (cgs), $\xi_{\rm t}$ = 2.2 km s^{-1}) and metallicity, for CH Cyg are approximately equal to those for normal M7 giants.

2. Although the orbital period of symbiotic system CH Cyg of ∼5300$^{\rm d}$ is not unusual as compared with orbital periods of barium stars (Jorissen et al. 1998)[1], CH Cyg does not display any abundance peculiarities in comparison with single field M giants. The calculated [C/H] = −0.15, [N/H] = +0.16, and [O/H] = −0.07 are close to the averaged values for six M giants, [C/Fe] = −0.14 ± 0.09, [N/Fe] = +0.44 ± 0.13 and [O/Fe] = −0.08 ± 0.08 analyzed by Smith & Lambert (1990). The isotopic ratios of $^{12}C/^{13}C$ and $^{16}O/^{17}O$ for CH Cyg are found to be 18^{+12}_{-6} and 830^{+400}_{-270}, respectively, in agreement with those for giants experiencing the first dredge-up. There is no signature of significant s-process enhancement, so synthesis of neutron-capture elements in WD progenitor (AGB star in the past) or mass transfer to the secondary (now primary) was not efficient. The reason of this could be high metallicity of the star, in agreement with the scenario proposed by Jorissen (2003, and references therein). By comparison the *yellow* symbiotic stars, which have significant enhancement of s-process elements, are metal-deficient.

3. The C/O ratio calculated for CH Cyg using the technique of emission lines provided by Nussbaumer et al. (1988) is close to that obtained from analysis of the absorption lines. However, results for C/N and O/N ratios derived from the two techniques are significantly different.

[1] Note that different chanels of mass transfer in binaries can produce barium (peculiar) stars with orbital periods from 10 to 400 000 days (Han et al. 1995).

4. The strong lines in the CH Cyg infrared spectrum are more shallow than those of standard M giants. This may reflect modification by high-energy radiation of the WD companion. In any case, abundances derived using strong (>300 mÅ) lines are sensitive to the atmospheric model.

Acknowledgements. This research was partly founded by KBN Research Grants Nos. 5 P03D 019 20, and 1 P03D 017 27. The collaborative program between Polish and Latvian Academy of Sciences is acknowledged for support. We thank the referee, Hans Martin Schmid, for important sugestions which improved the paper.

References

Bauschlicher, C. W. Jr., Langhoff, S. R., & Taylor, P. R. 1988, ApJ, 332, 531
Costes, M., Naulin, C., & Dorthe, G. 1990, A&A, 232, 270
Davis, S. P., & Phillips, J. G. 1963, The Red System of the CN molecule (Berkley and Los Angeles: Univ. Of California Press), 214
Dyck, H. M., Belle, G. T., & Thompson, R. R. 1999, AJ, 116, 981
ESA 1997, The Hipparcos and Tycho Catalogues, ESA SP-1200
Galazutdinov, G. 1992, Spec. Astr. Obs. Prepr., 92, 52
Goorvitch, D. 1994, ApJS, 95, 535
Goorvitch, D., & Chackerian, C., Jr. 1994, ApJS, 91, 483
Grevesse, N., & Sauval, A. J. 1998, Space. Sci. Rev., 85, 161
Hall, D. N. B., Ridgway, S. T., Bell, E. A., & Yarborough, J. M. 1978, Proc. SPIE, 172, 121
Han, Z., Eggleton, P. P., Podsiadlowski, P., & Tout, C. A. 1995, MNRAS, 277, 1443
Hauschildt, P. H., Allard, F., Ferguson, J., Baron, E., & Alexander, D. R. 1999, ApJ, 525, 871
Hinkle, K. H., Hall, D. N. B, & Ridgway, S. T. 1982, ApJ, 252, 697
Hinkle, K. H., Fekel, F. C., Johnson, D. S., & Scharlach, W. W. G. 1993, AJ, 105, 1074
Hinkle, K. H., Lebzelter, T., Joyce, R. R., & Fekel, F. C. 2002, AJ, 123, 1002
Hinkle, K., Wallace, L., & Livingston, W. 1995, PASP, 107, 1042
Houdashelt, M. L., Bell, R. A., Sweigart, A. V., & Wing, R. F. 2000, AJ, 119, 1424
Ivezić, Z., & Elitzur, M. 1995, ApJ, 445, 415
Ivezić, Z., & Elitzur, M. 1997, MNRAS, 287, 799
Jorissen, A. 2003, in Symbiotic stars probing stellar evolution, ed. R. L. M. Corradi, J. Mikołajewska, & T. J. Mahoney, ASP Conf. Ser., 303, 25
Jorissen, A., Smith, V. V., & Lambert, D. L. 1992, A&A, 261, 164
Jorissen, A., Van Eck, S., Mayor, M., & Udry, S. 1998, A&A, 332, 877
Keenan, P. C. 1963, in Basic Astronomical Data, ed. K. A. Strand (Chicago: University of Chicago Press), 78
Kupka, F., Piskunov, N., Ryabchikova, T. A., Stempels, H. C., & Weiss, W. W. 1999, A&AS, 138, 119
Kurucz, R. L. 1993, CD-ROM 13, Smithsonian Astrophys. Obs.
Kurucz, R. L. 1995, CD-ROM 18, Smithsonian Astrophys. Obs.
Melendez, J., & Barbuy, B. 1999, ApJS, 124, 527
Mikołajewska, J. 2001, in Small Telescope Astronomy on Global Scales, ed. B. Paczynski, W. P. Chen, & C. Lemme, ASP Conf. Ser., 246, 167
Mikołajewska, J., Selvelli, P. L., & Hack, M. 1988, A&A, 198, 150
Mikołajewska, J., Mikołajewski, M., & Selvelli, P. L. 1993, in Stellar Jets and Bipolar Outflows (Kluwer), ed. L. Errico, & A. A. Vittone, 155
Mikołajewski, M., Mikołajewska, J., & Khudyakova, T. N. 1992, A&A, 254, 127
Munari, U., Yudin, B. F., Kolotilov, E. A., & Tomov, T. V. 1996, A&A, 311, 484
Murset, U., & Schmid, H. M. 1999, A&AS, 137, 473
Nussbaumer, H., Schild, H., Schmid, H. M., & Vogel, M. 1988, A&A, 198, 179
Pereira, C. B., Smith, V. V., & Cunha, K. 1998, AJ, 116, 1977
Richichi, A., Fabbroni, L., Ragland, S., & Scholz, M. 1999, A&A, 344, 511
Schild, H., Dumm, T., Folini, D., Nussbaumer, H., & Schmutz, W. 1999, in The Universe as seen by ISO, ed. P. Cox, & M. F. Kessler, ESA SP-427, 397
Schmid, H. M. 1994, A&A, 284, 156
Smith, V. V., & Lambert, D. L. 1985, ApJ, 294, 326
Smith, V. V., & Lambert, D. L. 1990, ApJS, 72, 387
Smith, V. V., Cunha, K., Jorissen, A., & Boffin, H. M. J. 1996, A&A, 315, 179
Smith, V. V., Cunha, K., Jorissen, A., & Boffin, H. M. J. 1997, A&A, 324, 97
Smith, V. V., Pereira, C. B., & Cunha, K. 2001, ApJ, 556, L55
Sneden, C. 1973, ApJ, 184, 839
Vanture, A. D., Wallerstein, G., Gallino, R., & Masera, S. 2003, ApJ, 587, 2003
Wallace, L., & Hinkle, K. 1996, ApJS, 107, 312
Wallace, L., Livingston, W., & Hinkle, K. 1996, ApJS, 106, 165
Wood, P. R., Olivier, E. A., & Kawalar, S. D. 2004, ApJ, 604, 800
Začs, L. 2000, The chemical composition and orbital parameters of barium stars. In Proceedings of the 177th Symposium of IAU, ed. R. F. Wing (Dordrecht: Kluwer), 277

Online Material

Table 1. gf-values, excitation potentials and averaged equivalent widths of atomic lines in the spectra of CH Cyg and the Sun.

Wavelength (Å)	*EP* (eV)	log gf	Sun (mÅ)	CH Cyg (mÅ)	Wavelength (Å)	*EP* (eV)	log gf	Sun (mÅ)	CH Cyg (mÅ)
Mg I					Fe I				
15 952.74	6.59	–1.98	8	228	16 233.10	6.38	–1.18	7	38
16 629.27	6.73	–1.77		266	16 247.52	6.28	–1.09	14	54
16 636.57	6.73	–1.51		224	16 263.37	6.24	–0.90	20	102
17 090.30	6.73	–1.92	11	258	16 281.95	6.32	–0.51	38	113
17 754.47	6.73	–1.75	8	210	16 323.17	5.92	–0.60	74	173
17 758.55	6.73	–1.78		242	16 441.12	5.92	–0.56	82	156
17 758.60	6.73	–1.47		242	16 444.91	6.29	–0.36	67	148
17 766.91	6.73	–1.11		300	16 520.18	5.56	–2.41	3	48
21 065.48	6.78	–1.55		213	16 526.05	6.29	–0.67	35	103
21 231.38	6.73	–1.32	33	278	16 656.78	6.34	–0.65	34	125
Si I					16 683.73	5.92	–1.05	34	164
15 642.74	6.73	–1.76	10	35	16 697.67	6.42	–0.41	40	140
15 805.27	6.80	–1.60	06	21	16 726.03	6.38	–0.52	36	166
16 064.41	5.95	–0.66	279	239	16 815.97	6.30	–1.02	14	57
16 099.20	5.96	–0.25		301	16 904.85	6.30	–1.27	9	45
16 384.61	5.86	–1.00	194	246	16 915.31	5.87	–1.94	4	42
17 332.10	6.62	0.30		276	17 025.41	5.07	–2.48	6	110
20 922.86	6.73	0.69	418	280	17 126.29	5.94	–1.95	3	48
20 931.86	6.73	–0.86	41	66	17 493.34	6.41	–0.78	28	96
21 360.03	6.22	0.08	408	302	17 575.26	6.73	–0.17	28	97
21 785.60	6.72	0.55	304	213	17 586.72	6.38	–0.55	42	90
21 825.63	6.72	0.26	235	218	17 705.69	6.34	–0.98	15	96
21 880.11	6.72	–0.52	85	100	17 719.21	6.58	–0.64	14	96
21 885.30	6.72	0.52	311	220	20 953.87	6.12	–0.87	20	136
Ti I					21 183.92	3.02	–4.17	9	237
17 022.68	4.51	0.37	4	168	21 244.23	4.96	–1.38	77	258
17 381.32	4.49	0.33	4	147	21 290.17	3.07	–4.37	4	244
17 387.85	4.47	0.23	4	153	21 741.42	6.18	–0.65	27	111
17 393.26	4.51	0.48	7	216	21 819.72	5.85	–1.58	7	63
21 158.08	4.86	0.52	2	124	21 857.36	3.64	–3.91	9	196
21 314.43	3.89	–0.84	3	157	22 391.13	5.32	–1.53	23	146
21 872.05	3.92	–0.62		163	22 399.16	5.10	–1.26	67	191
Fe I					22 426.14	6.22	–0.17	62	139
15 643.22	5.81	–1.81	7	33	22 818.80	5.79	–1.26	21	105
15 674.41	6.20	–1.04	16	86	22 852.17	5.83	–0.67	69	224
15 675.28	6.33	–0.57	32	69					
15 704.38	6.33	–1.08	9	46	Ni I				
15 756.01	6.36	–0.85	11	63	16 037.88	6.20	–0.70	3	30
15 820.95	5.96	–0.73	55	120	16 140.51	5.49	–0.24	53	145
15 826.03	5.64	–0.96	58	161	16 367.58	5.28	0.28	165	310
15 844.52	6.36	–0.40	46	83	16 593.97	5.47	–0.59	27	184
15 862.99	5.59	–1.34	29	129	16 710.63	6.03	–0.97	2	41
15 900.89	6.34	–0.89	12	95	16 820.06	5.30	–0.70	29	205
15 933.83	6.31	–0.59	33	116	17 005.67	5.49	0.15	107	226
15 956.99	6.34	–0.81	26	99	17 311.29	5.49	–0.63	22	169
16 017.24	5.59	–1.97	8	56	17 365.45	6.07	–0.29	13	109
16 033.80	6.35	–0.63	31	75	17 898.76	6.10	–0.27		86
16 176.34	6.38	–0.52	33	113	17 993.39	6.10	0.01		161
16 182.44	6.38	–0.52	34	85	21 575.89	5.30	–1.32	10	113

Table 2. gf-values, excitation potentials and equivalent widths of molecular lines in the spectrum of CH Cyg.

Wavelength (Å)	χ (eV)	log gf	EW (mÅ)	Line	Wavelength (Å)	χ (eV)	log gf	EW (mÅ)	Line
OH					CO				
17 054.7187	1.10	–4.65	394	(4–2) P_2-9.5	16 285.845	1.5986	–5.7660	183	(6–3) R59
17 056.8417	1.10	–4.65	409	(4–2) P_2+9.5	16 300.055	0.5707	–7.1392	270	(5–2) P13
17 074.1425	1.10	–4.65	346	(4–2) P_1-10.5	16 301.731	1.6533	–5.7402	261	(6–3) R61
17 099.2187	0.84	–5.01	373	(2–0) P_1+18.5	16 310.142	1.6814	–5.7275	214	(6–3) R62
17 109.3710	0.96	–4.64	409	(3–1) P_1-15.5	16 310.965	2.0492	–5.8204	165	(5–2) R81
17 111.8320	0.84	–5.01	427	(2–0) P_1+19.5	16 312.011	0.7920	–7.1364	203	(6–3) R 4
17 114.9355	0.96	–4.64	446	(3–1) P_1+15.5	23 091.567	1.4401	–4.9234	373	(2–0) R78
17 320.8769	1.03	–4.59	442	(3–1) P_1+16.5	23 103.397	1.4763	–4.9147	355	(2–0) R79
17 338.7148	0.93	–4.97	379	(2–0) P_1+19.5	23 115.676	1.5128	–4.9062	305	(2–0) R80
17 590.4589	1.01	–4.92	405	(2–0) P_1-20.5	23 128.407	1.5499	–4.8979	318	(2–0) R81
17 594.9785	1.01	–4.92	456	(2–0) P_1-21.5	HF				
17 597.3300	1.01	–4.92	310	(2–0) P_1+20.5	23 364.7589	0.48	–3.9547	514	(1–0) R 9
17 603.7734	1.01	–4.92	335	(2–0) P_1+21.5	22 964.2745	0.71	–3.9393	332	(1–0) R13
17 612.1152	1.24	–4.42	289	(4–2) P_2-12.	22 893.0391	0.78	–3.9431	334	(1–0) R14
17 623.7226	1.24	–4.42	300	(4–2) P_1-13.5	22 784.5448	0.93	–3.9626	265	(1–0) R16
CN					$^{13}C^{16}O$				
21 911.0848	1.13	–1.87	86	(0–2) $Q_1$57	23 655.522	0.09	–5.73	584	(2–0) R19
21 934.7310	0.89	–2.28	54	(0–2) $P_1$47	23 605.117	1.45	–4.94	245	(2–0) R80
21 941.1191	0.89	–2.14	79	(1–3) $P_1$34	23 595.911	0.14	–5.62	514	(2–0) R24
21 942.6244	0.91	–2.13	85	(1–3) $P_2$35	23 486.772	0.32	–5.40	564	(2–0) R37
21 945.2729	1.07	–1.69	104	(0–2) $Q_1$44	23 475.782	0.35	–5.37	457	(2–0) R39
21 895.4928	1.07	–1.71	108	(0–2) $Q_2$44	23 473.000	0.94	–5.08	387	(2–0) R64
21 923.8628	1.37	–1.88	53	(2–4) $R_2$57	23 470.918	0.37	–5.36	492	(2–0) R40
21 956.4998	0.94	–2.37	59	(2–4) $P_2$18	23 466.497	0.39	–5.34	462	(2–0) R41
21 914.6381	0.99	–1.89	82	(2–4) $Q_1$23	23 460.072	0.85	–5.11	380	(2–0) R61
21 939.3027	1.02	–1.85	85	(2–4) $Q_2$26	$^{12}C^{17}O$				
21 943.5874	1.20	–1.94	94	(2–4) $R_1$38	23 358.509	0.15	–5.58	162	(2–0) R25
21 926.9394	1.22	–1.94	75	(2–4) $R_2$39	23 338.271	0.18	–5.54	174	(2–0) R27
CO					23 311.069	0.22	–5.49	207	(2–0) R30
16 163.720	0.3464	–7.4573	257	(4–1) P18	23 328.945	0.19	–5.53	164	(2–0) R28
16 178.560	0.3554	–7.4383	220	(4–1) P19	23 319.865	0.20	–5.51	193	(2–0) R29
16 266.752	0.8128	–6.7650	286	(6–3) R10	23 302.812	0.23	–5.48	142	(2–0) R31
16 278.366	1.5718	–5.7791	261	(6–3) R58	23 295.035	0.24	–5.46	147	(2–0) R32
16 280.684	0.8040	–6.8620	226	(6–3) R 8	23 287.433	0.26	–5.44	144	(2–0) R33